Contents lists available at ScienceDirect

Computational Materials Science

Graphene heals thy cracks

Sanghamitra Debroy [a], V. Pavan Kumar Miriyala [a], K. Vijaya Sekhar [b], Swati Ghosh Acharyya [b,*], Amit Acharyya [a]

[a] Department of Electrical Engineering, Indian Institute of Technology, Hyderabad, India
[b] School of Engineering Sciences and Technology, University of Hyderabad, India

ARTICLE INFO

ABSTRACT

Molecular Dynamics simulations revealed the phenomena of self healing of cracks which were generated in graphene on application of tensile load exceeding its ultimate tensile strength. The phenomenon of self healing was observed when the system was studied at a very slow rate of 0.05 ps. Cracks initiated in the graphene sheet was allowed to propagate till it reached a critical length following which the load was removed and the sheet was relaxed. The study revealed that self healing of cracks took place within a critical crack opening displacement range of 0.3–0.5 nm in absence of any external stimulus. However, the self healing phenomenon was found to be independent of crack length. This self healing phenomenon occurred not only in pristine graphene sheet, but also in presence of pre-existing vacancies. The mechanism of self healing has been explained by detailed bond length/angle distribution analysis.

© 2015 Published by Elsevier B.V.

1. Introduction

The exceptional band structure of graphene bestows it with extraordinary electrical transport properties, owing to which it is believed to be an immensely potential candidate for next generation electronics [1–9]. Unlike two-dimensional electron layers in semiconductors, where the charge carriers become immobile at low densities, the carrier mobility in graphene can remain high, even when their density vanishes at the Dirac point [10]. The ultra-high mobility and large saturation velocity of graphene makes it a promising candidate for low power consumption and high speed electronics [11–14]. However, one of the major challenges in application of graphene for low power electronics is imposed by the presence of defects in graphene fabricated real time such as cracks, vacancies and Stone–Wales defects [15–17]. Defects in graphene, especially cracks have shown to affect both the mechanical and electrical properties of graphene significantly [18]. This has led to numerous studies on understanding the fracture behaviour of graphene [19–24]. The fracture toughness of graphene as reported by several researchers both from experimental and theoretical studies is found to be as low as 4.0 ± 0.6 MPa$\sqrt{m}$ [24] and hence forms a critical hurdle in its all-round application. In this regard self healing of defects in graphene holds great significance and thus has received lot of attention by the researchers [25–32].

Formerly, it has been reported both from experimental studies and also by Molecular Dynamics simulations that graphene can heal its vacancy defects and other topological defects with the aid of metal doping [25–32]. However 'self healing of cracks' has not been reported till date to the best of the authors' knowledge perhaps because the healing of crack takes place so fast (~few pico seconds) that it cannot be captured even by the high-end microscopes. We hereby report for the first time the phenomenon of self healing of cracks in graphene without the presence of any external stimulus at room temperature.

The convention used in the present study for direction of graphene sheet is shown in Fig. 1(A). Longitudinal mode (LM): tensile load is parallel to C–C bond direction. Transverse mode (TM): load is normal to C–C bond direction. Fig. 1(B) shows a typical crack in graphene sheet with crack length and crack opening displacement labeled.

The cracks in graphene sheet can be referred to as *cracks* which have been generated in the graphene sheet during application of tensile load. In our study, self-healing phenomenon has been reported for cracks. Moreover, self healing phenomenon has been found to hold true even in presence of defects like single vacancy in the graphene sheet. The cracks which propagated throughout the width of the graphene sheet also healed once the load was relaxed.

2. Methods

2.1. Atomistic modelling

The MD simulations in the present study were performed using LAMMPS [33] (Large-scale Atomic/Molecular Massively parallel

* Corresponding author.
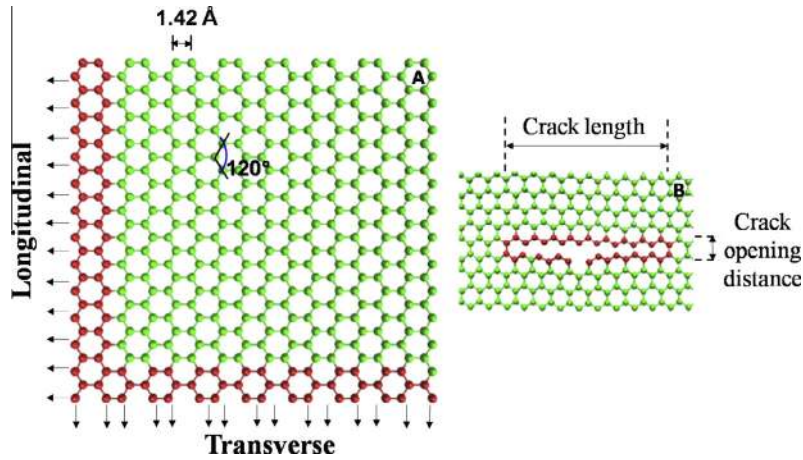E-mail address: sgase@uohyd.ernet.in (S. Ghosh Acharyya).

Fig. 1. (A) Conventions used for loading of graphene sheet and bond length bond angle for pristine sheet. (B) Crack length and crack opening displacement.

simulator). We used AIREBO (Adaptive inter-molecular reactive Bond order potential) to define force field to our simulation model which originated from Tersoff–Berner potential, which defines bond–bond interactions, bond breaking, bond reforming, inter molecular interactions between non-bonded atoms, as well as torsion angles formed by the sequence of three bonds [34,35]. In order to limit the many body bond-order potential to nearest neighbour interactions, a cut-off function was used. In fracture studies, this plays a crucial role, inducing high bond order forces resulting in deviation from physical behaviour. In the present study, we had set the cut-off to 2 Å, eliminating non-physical ductile behaviour in stretching process and to get accurate fracture behaviour.

We implemented quantized fracture mechanics (QFM) modified Griffith's model. Based on QFM modelling, the fracture strength is largely related to crack tip radius and crack length and is accurate in studying fracture behaviour, previously proved by [36,37]. The quantised fracture strength is given by the following equation:

$$\sigma_f(l, \rho) = \sigma_c \sqrt{\frac{1 + \rho/2L_0}{1 + 2l/L_0}} \qquad (1)$$

where σ_c is fracture strength of pristine sheet, ρ is crack tip radius, l is crack length, L_0 is minimum propagation distance of the crack. The simulations were performed on $(5 \times 5 \text{ nm})$ graphene sheet which contained 1008 carbon atoms with PBC boundary conditions in two in-plane directions and a vacuum space of 100 nm was considered alongz-direction to avoid edge effects. All simulations were performed at 300 K room temperature by Nose–Hoover thermostat. The Velocity-Verlet time integrating scheme was applied with a time step of 0.0005 ps and held at equilibrium for 30 ps. After equilibrium was attained, tensile test had been carried out by deformation control method by applying strain loading with an increment of 0.001/ps till the ultimate tensile strength of the material was reached. In order to study self-healing phenomenon, all the forces acting on the deformed graphene sheet were removed and the sheet was allowed to relax for a period of 150 ps.

3. Results

We performed Molecular Dynamics simulations for the mechanical properties of defect free graphene assuming it's thickness to be 3.4 Å [38]. Nominal fracture strengths are identified as 89 GPa at 0.14 and 105 GPa at 0.215 fracture strain, respectively for longitudinal mode and transverse mode, which is exactly at

par with previous studies and in agreement with experimental results [38–42] thereby validating the accuracy of our model.

In order to study the self-healing of cracks in graphene sheet $(5 \times 5 \text{ nm})$ we have classified this present work into four different categories i.e. (a) pristine condition, longitudinal loading direction, (b) pristine condition, transverse loading direction and (c) presence of single vacancy defect, longitudinal loading direction [43,44]. The simulations have been carried out at constant room temperature $T = 300 \text{ K}$, in the canonical ensemble (NVT), where amount of substance (N), volume (V) and temperature (T). To reach the equilibrium thermodynamic state at this constant temperature, the Nose–Hoover thermostat with Velocity-Verlet integration algorithm is also implemented. Applying this thermostat method produces lesser instabilities in the system throughout the temperature stabilization process. Periodic Boundary Conditions are imposed on the system and allowed to relax for a period of 30 ps. The cracks are formed and are propagated in the pristine sheets by uniaxial loading with constant strain rate of 0.001/ps after reaching the ultimate tensile strength.

Once the graphene sheet completely fails it is then relaxed for a period 30 ps by removing all forces acting on it at room temperature. The simulation as listed above were repeated for different crack lengths and crack opening displacements in order to determine the critical value in each case and it was observed that when the crack opening displacement is within a range of 0.3–0.5 nm, the cracks heals thyself. The results obtained in each case are detailed as follows.

The phenomenon of self healing of cracks in graphene was verified in both pristine and defected graphene sheet. Fig. 2A–D shows the different stages of self healing for pristine sheet in longitudinal mode. Bond angle and bond length distribution analysis was done to get a clear picture in each case at different stages of the self healing phenomenon represented in Fig. 2E–L. Self-healing of cracks was also observed for pristine sheet under transverse mode of loading and the different stages of self healing is shown in Fig. 3A–D. The bond angle and bond length distribution analysis for this case is given in Fig. 3E–L.

In the third case, a graphene sheet containing a vacancy had been used as a starting material and tensile load was applied to the sheet. Once the ultimate tensile strength of the material was exceeded, the cracks nucleated in the region of the vacancy and extended throughout the sheet as shown in Fig. 4A–E. Once the load was relaxed, the cracks were found to heal in 5.6 ps and only the vacancy defect created initially remained as unaltered. This is due to the fact that the vacancy defect was created by
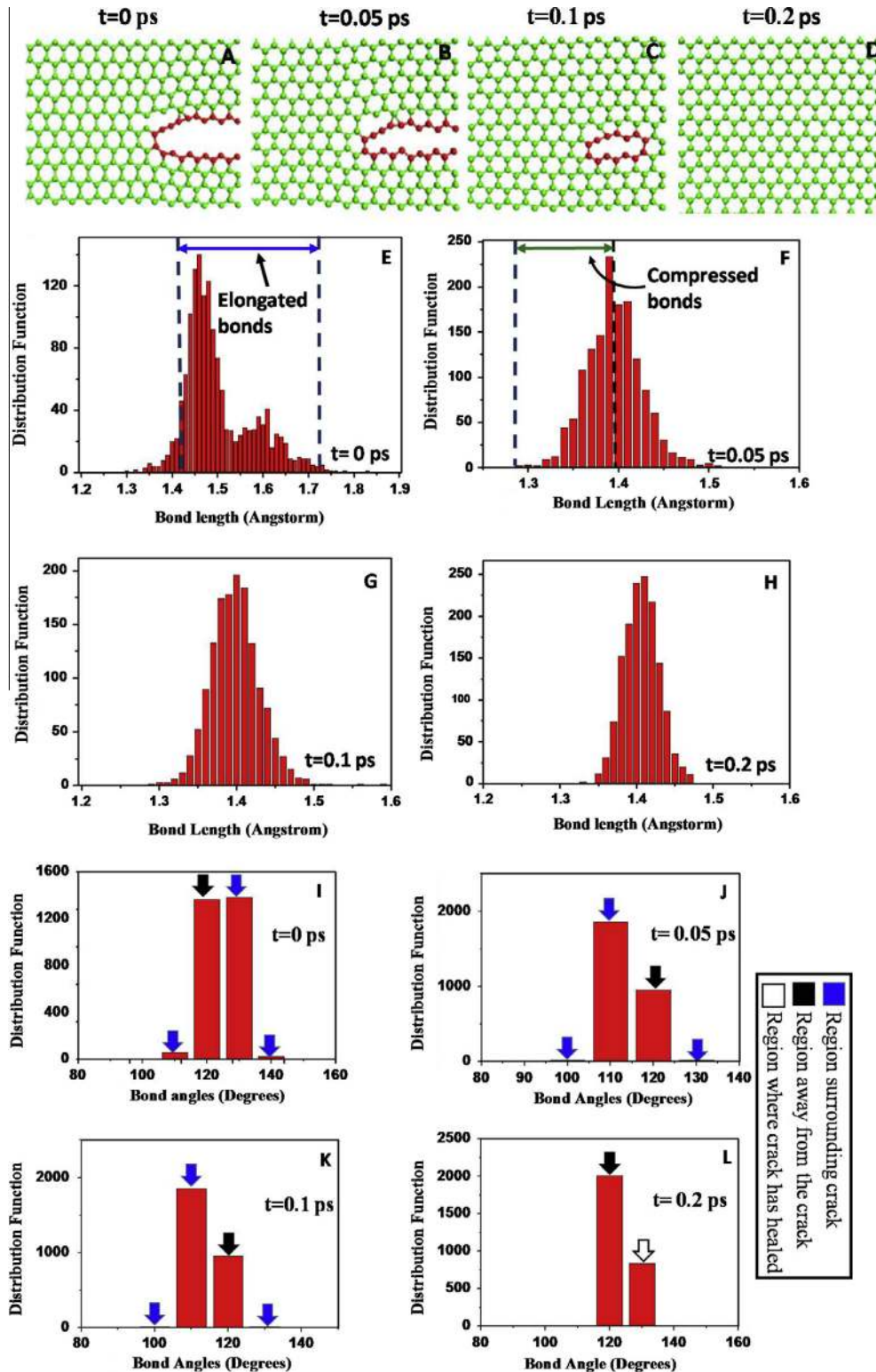
Fig. 2. (A–D) Shows the different stages of self-healing for pristine sheet in longitudinal mode. (E–H) Bond length distribution analysis for different stages of self-healing for pristine sheet in longitudinal mode. (I–L) Bond angle distribution analysis for different stages of self-healing for pristine sheet in longitudinal mode.

deleting atoms in the graphene sheet. Moreover, the canonical ensemble did not contain any extra atoms which could fill in the vacancy.

It was further observed that in some cases, the healed sheet of graphene contained some Stone Wales defect formed as a result of

the atomic rearrangement occurring during the healing stage. The healed sheet of graphene containing Stone Wales defect is shown in Fig. 5. Fig. 5A shows the resultant sheet for the case of pristine sheet loaded longitudinally and Fig. 5B showed the resultant sheet for the case of graphene sheet focused near a vacancy defect.
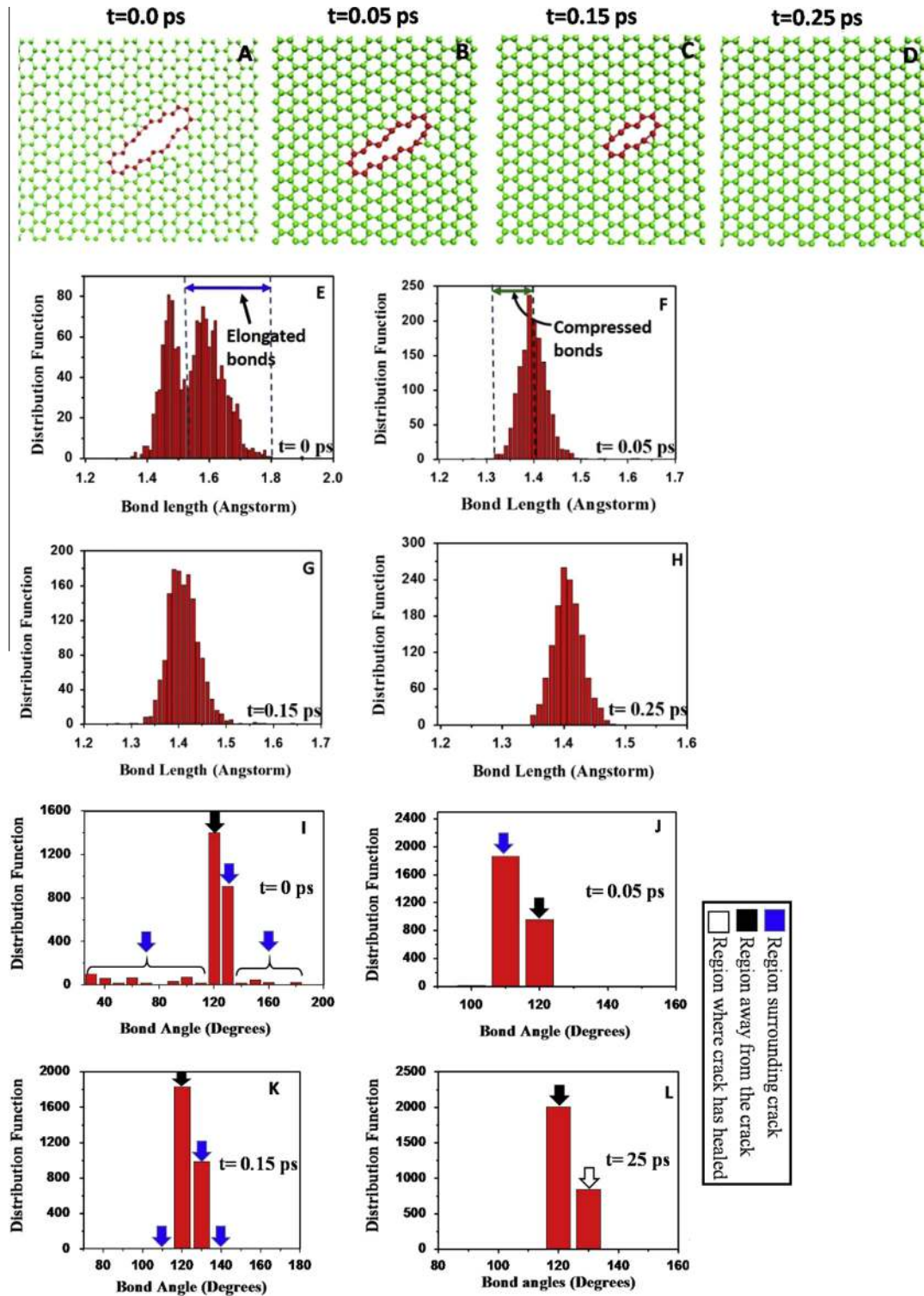
Fig. 3. (A–D) Shows the different stages of self-healing for pristine sheet in transverse mode. (E–H) Bond length distribution analysis for different stages of self-healing for pristine sheet in transverse mode. (I–L) Bond angle distribution analysis for different stages of self-healing for pristine sheet in transverse mode.

4. Discussion

4.1. Understanding the phenomenon of self-healing of cracks in graphene

In case of pristine graphene sheet loaded in longitudinal direction at relaxation time $t = 0$ ps (Fig. 2A) i.e. at the point of removal of loads and relaxation of the sheet, it was perceived that 91% of the bond lengths were found to be elongated in the range of 1.43–1.78 Å and 51% of bond angles were in the range of 130–180°, as compared to the bond length of 1.42 Å and bond angle of 120° of pristine graphene. The scattering of bonds length/angles at different stages of self healing has been shown in Fig. 2E–L. At around $t = 0.05$ ps after relaxation, 74% of the bond lengths were
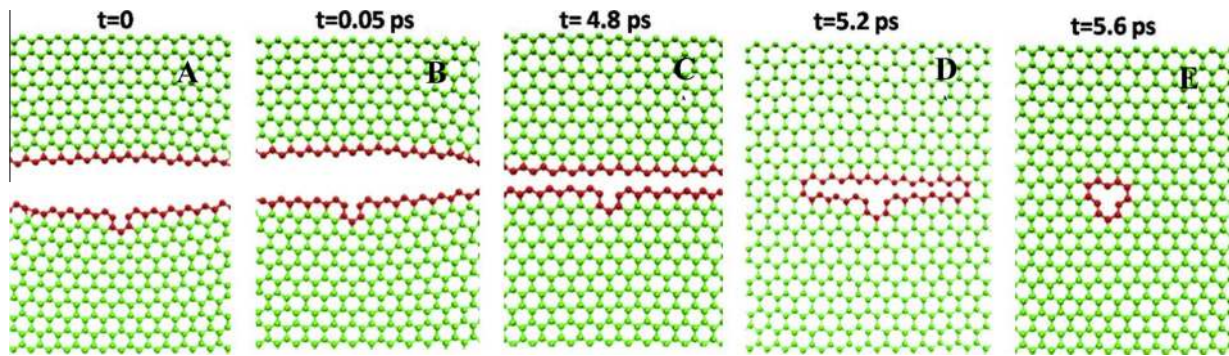
Fig. 4. (A–E) Different stages of self-healing for graphene sheet with single vacancy defect in longitudinal mode.
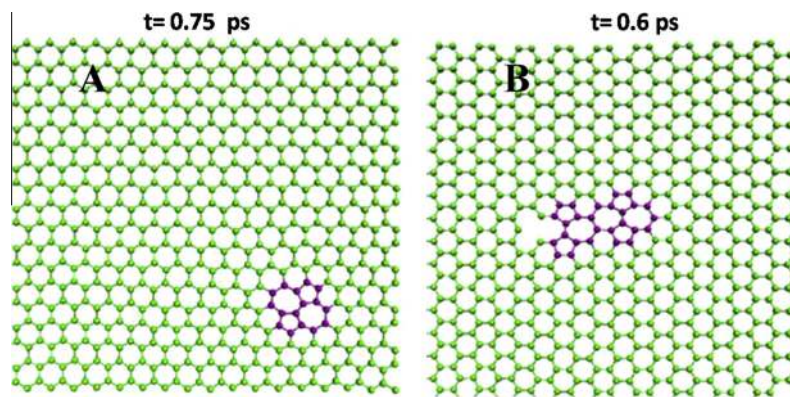

Fig. 5. Stone Wales defect formed in the healed sheet of graphene in (A) pristine sheet and (B) in surroundings of a vacancy defect.

reduced to the range of 1.3–1.4 Å and 66% of angles reduced to the range of 70–110°.

Hence once the tensile stresses were removed, the graphene sheet contracted by virtue of its elastic behaviour [45,46] and the C atoms moved closer to each other. Hexagonal rings of C atom were distorted as evident by the reduction in the bond angle. At $t = 0.1$ ps, 19% of the bond lengths were back in the range of 1.43–1.48 Å and 34% of angles were in the range of 120–130° indicating a relaxation from the stage of compression. In this stage the re-bonding of the dangling bonds was observed resulting in the formation of pentagonal defects. These defects then coalesced forming longer C chains in 0.05 ps, and the original hexagonal ring structure of carbon atoms as present in pristine sheet was obtained after 0.2 ps. This finally led to selfhealing of crack in graphene sheet. However the rearrangement of atomic bonds continued in the graphene sheet leading to the formation of Stone Wales defects in the sheet (Fig. 5) as observed after $t = 0.75$ ps. In order to confirm healing occurred in the pristine graphene sheet, tensile testing of the healed graphene sheet was carried on, and the fracture strength observed was 75 GPa i.e. about 16% less as compared to the pristine graphene sheet. The reduction in the value of fracture stress is owing to the formation of Stone Wales defect in the healed sheet. This proves that the graphene sheet can be reused repetitively but with certain degradation in the quality of the sheet.

The bond angle/length distribution analysis for transverse mode of loading also showed similar behaviour wherein the sheet got compressed initially on releasing load and then self-healing of crack took place. Finally the atomic rearrangements in the graphene sheet lead to the formation of Stone Wales defect on reaching the equilibrium state. In this case approximately 90% of the bond length were elongated in the range of 1.43–1.78 Å and bond angles were stretched almost 35% between 120° and 180° leading to the cracked structure shown in Fig. 3E–L. At final stage, within nearly a time period 0.25 ps all the crack were healed (Fig. 3D) with almost 21% of the bond lengths in the range of 1.43–1.48 Å and 30% bond angles between 120° and 130°.

4.2. Effect of pre-existing vacancy on self-healing of cracks

The case of graphene sheet containing single vacancy defect is shown in Fig. 4. The cracks nucleated from the region of the pre-existing defect on application of tensile loading. On relieving the load, the cracks were found to self-heal with time in a similar way as discussed above for the case of pristine sheet of graphene. However, the time taken to heal the crack is more in case of a pre-existing defect than in case of a pristine sheet.

4.3. Critical crack opening displacement

In all of the cases discussed above, the study was repeated with different values of crack length and crack opening displacement so as to arrive at the critical crack length and crack opening displacement required for self healing to occur. The results indicated that the phenomenon of self-healing was independent of the length of the crack hence cracks of any length would be healed once the load is relaxed and thus defining critical crack length is not needed. However, the critical crack opening displacement was found to 0.3–0.5 nm i.e. the distance between the crack surfaces should be within 0.5 nm for the cracks to be healed. If the crack opening displacement exceeded 0.5 nm, self healing of the cracks would not take place.

5. Conclusion

Molecular Dynamics simulation was carried on to study self-healing of cracks in graphene in pristine condition and in presence of pre-existing vacancy defect. Detailed analyses of the deformation present in the sheet were done using bond length and bond angle distribution analysis. The findings of the study are summarized as follows:

(a) Cracks nucleated in graphene sheet on application of uniaxial tensile load exceeding its ultimate tensile strength self-heal on removal of all loads acting on it.
(b) The phenomenon of self-healing has been found to be independent of crack length i.e. long cracks propagating throughout the graphene sheet has been found to heal on relaxation of load. Critical crack opening displacement range of 0.3–0.5 nm needs to be met for self healing to occur. If crack opening displacement exceeds this limit no healing is found to occur.
(c) Bond length and bond angle distribution analysis revealed that healing took place due to the elastic nature of graphene.
(d) The resultant sheets of graphene post self healing of cracks were found to contain some Stone Wales defects.

Author contributions

V.P.K., S.D. and K.V.S. carried out the Molecular Dynamics simulations and prepared the figures. S.D. wrote the paper. S.G.A. and A.A. supervised the project and revised the paper. All authors discussed the results and commented on the manuscript.

Supplementary materials

All the important findings are uploaded in terms of animations on my webpage to give a feel of the work: http://www.iith.ac.in/~amit_acharyya/photo_gal.html.

References

[1] A.K. Geim, K.S. Novoselov, Nat. Mater. 6 (2007) 183–191, http://dx.doi.org/10.1038/nmat1849.
[2] K.I. Bolotin, K.J. Sikes, J. Hone, H.L. Stormer, P. Kim, Phys. Rev. Lett. 101 (2008) 096802, http://dx.doi.org/10.1103/PhysRevLett.101.096802.
[3] L. Chenguang, Y. Zhenning, N. David, Z. Aruna, J. Bor, Nano Lett. 10 (2010) 4863–4868, http://dx.doi.org/10.1021/nl102661q.
[4] A.H. Castro Neto, F. Guinea, N.M.R. Peres, K.S. Novoselov, A.K. Geim, Rev. Mod. Phys. 81 (2009) 109, http://dx.doi.org/10.1103/RevModPhys.81.109.
[5] W. Qiong, X. Yuxi, Y. Zhiyi, L. Anran, S. Gaoquan, Nano Lett. 4 (2010) 1963–1970, http://dx.doi.org/10.1021/nn1000035.
[6] Y.M. Lin et al., Nano Lett. 9 (2009) 422–426, http://dx.doi.org/10.1021/nl803316h.
[7] L. Lei et al., Nature 467 (2010) 305–308, http://dx.doi.org/10.1038/nature09405.
[8] S. Roman, T. Floriano, R. Valeria, Appl. Phys. Lett. 94 (2009) 073305, http://dx.doi.org/10.1063/1.3079663.
[9] J.W. Kang, K.W. Lee, Comput. Mater. Sci. 93 (2014) 164–168, http://dx.doi.org/10.1016/j.commatsci.2014.06.041.
[10] K.I. Bolotin et al., Solid State Commun. 146 (2008) 351–355, http://dx.doi.org/10.1016/j.ssc.2008.02.024.
[11] C.H. Yeh et al., Nano Lett. 8 (2014) 7663–7670, http://dx.doi.org/10.1021/nn5036087.
[12] Q. Mao et al., Opt. Lett. 39 (2014) 5649–5652, http://dx.doi.org/10.1364/OL.39.005649.
[13] D. Turchinovich et al., Int. Conf. Ultrafast Phenom. 07 (2014) 7–11, http://dx.doi.org/10.1364/UP.2014.09.Wed.B.4.
[14] Y.M. Lin et al., Science 327 (2010) 662, http://dx.doi.org/10.1126/science.1184289.
[15] O. Frank et al., Nano Lett. 12 (2012) 687–693, http://dx.doi.org/10.1021/nl203565p.
[16] D.W. Boukhvalov, M.I. Katsnelson, Nano Lett. 8 (2008) 4373–4379, http://dx.doi.org/10.1021/nl802234n.
[17] A. Lherbier et al., Phys. Rev. Lett. 106 (2011) 046803, http://dx.doi.org/10.1103/PhysRevLett.106.046803.
[18] N. Gorjizadeh, A. Farajian, Y. Kawazoe, Nanotechnology 20 (2009) 015201, http://dx.doi.org/10.1088/0957-4484/20/1/015201.
[19] H. Zhao, N.R. Aluru, J. Appl. Phys. 108 (2010) 064321, http://dx.doi.org/10.1063/1.3488620.
[20] M.Q. Le, R.C. Batra, Comput. Mater. Sci. 84 (2014) 238–243, http://dx.doi.org/10.1016/j.commatsci.2013.12.007.
[21] M.Q. Le, R.C. Batra, Comput. Mater. Sci. 69 (2013) 381–388, http://dx.doi.org/10.1016/j.commatsci.2012.11.057.
[22] T.C. Theodosiou, D.A. Saravanos, Comput. Mater. Sci. 82 (1) (2014) 56–65, http://dx.doi.org/10.1016/j.commatsci.2013.09.032.
[23] Y.Y. Zhang, Y.T. Gu, Comput. Mater. Sci. 71 (2013) 197–200, http://dx.doi.org/10.1016/j.commatsci.2013.01.032.
[24] Z. Peng et al., Nat. Commun. 5 (2014) 3782, http://dx.doi.org/10.1038/ncomms4782.
[25] R. Zan, Q.M. Ramasse, U. Bangert, K.S. Novoselov, Nano Lett. 12 (2012) 3936–3940, http://dx.doi.org/10.1021/nl300985q.
[26] L. Tsetseris, S.T. Pantelides, Carbon 47 (2008) 901–908, http://dx.doi.org/10.1016/j.carbon.2008.12.002.
[27] V.O. Özçelik, H.H. Gurel, S. Ciraci, Phys. Rev. B 88 (2013) 045440, http://dx.doi.org/10.1103/PhysRevB.88.045440.
[28] L. Yung-Chang, Y. Chao-Hui, H. Ju-Chun, C. Po-Wen, Nano Lett. 6 (2012) 4469–4474, http://dx.doi.org/10.1021/nn301199j.
[29] J. Chen et al., Appl. Phys. Lett. 102 (2013) 103107, http://dx.doi.org/10.1063/1.4795292.
[30] D.Y. Kim et al., Adv. Funct. Mater. 24 (2014) 4986–4995, http://dx.doi.org/10.1002/adfm.201400732.
[31] X. Xingcheng, C. Tao, C. Yang-Tse, J. Mater. Chem. 20 (2010) 3508–3514, http://dx.doi.org/10.1039/C0JM00307G.
[32] C. Hou et al., Sci. Rep. 3 (2013) 3138, http://dx.doi.org/10.1038/srep03138.
[33] S. Plimpton, J. Comput. Phys. 117 (1995) 1–19, http://dx.doi.org/10.1006/jcph.1995.1039.
[34] S.J. Stuart, A.B. Tutein, J.A. Harrison, J. Chem. Phys. 112 (2000) 6472–6486, http://dx.doi.org/10.1063/1.481208.
[35] J. Tersoff, Phys. Rev. B 37 (1988) 6991, http://dx.doi.org/10.1103/PhysRevB.37.6991.
[36] D.W. Brenner, Phys. Rev. B 46 (1948) 1992, http://dx.doi.org/10.1103/PhysRevB.46.1948.2.
[37] S. Nose, J. Chem. Phys. 81 (1984) 511–519, http://dx.doi.org/10.1063/1.447334.
[38] J. Zhu, M. He, F. Qiu, Chinese J. Chem. 10 (2012) 1399–1404, http://dx.doi.org/10.1002/cjoc.201200505.
[39] H. Zhao, K. Min, N.R. Aluru, Nano Lett. 9 (2009) 3012–3015, http://dx.doi.org/10.1021/nl901448z.
[40] M.C. Wang, C. Yan, L. Maa, N. Hu, Comput. Mater. Sci. 68 (2013) 138–141, http://dx.doi.org/10.1016/j.commatsci.2012.09.035.
[41] C. Lee, X. Wei, J.W. Kysar, J. Hone, Science 321 (2008) 385–388, http://dx.doi.org/10.1126/science.1157996.
[42] Y. Zheng, N. Wei, Z. Fan, L. Xu, Z. Huang, Nanotechnology 22 (2011) 405701, http://dx.doi.org/10.1088/0957-4484/22/47/479501.
[43] M.A.N. Dewapriya, R.K.N.D. Rajapakse, J. Appl. Mech. 81 (2014) 1159, http://dx.doi.org/10.1115/1.4027681.
[44] R. Ansari, S. Ajori, B. Motevalli, Superlattices Microstruct. 51 (2012) 274–289, http://dx.doi.org/10.1016/j.spmi.2011.11.019.
[45] C.G. Navarro, M. Burghard, K. Kern, Nano Lett. 8 (2008) 2045–2049, http://dx.doi.org/10.1021/nl801384y.
[46] K.H. Kim, Y. Oh, M.F. Islam, Nat. Nanotechnol. 7 (2012) 562–566, http://dx.doi.org/10.1038/nnano.2012.118.